

Two-Center, Three-Center, and Four-Center Dative π -Bonding Systems in Boron–Nitrogen Compounds Studied by Density Functional Theory Calculations: The Molecular Structures of Bis(dimethylboryl)amine, Bis(dimethylboryl)methylamine and Bis(dimethylamino)methylborane Determined by Gas Electron Diffraction

Kari-Anne Østby, Arne Haaland,* and Grete Gundersen*

Department of Chemistry, University of Oslo, Box 1033 Blindern, N-0315 Oslo, Norway

Heinrich Nöth

Institute of Inorganic Chemistry, Ludwig-Maximilians-Universität München, Butenandtstrasse 7-13, Haus D, D-81377 München, Germany

Received June 10, 2005

The nature of the two-center, two-electron (2c,2e) dative π -bonding system in aminoboranes has been explored by optimizing the equilibrium structures of $R_2NBR'_2$ ($R, R' = H$ or Me) by DFT calculations at the B3PW91/6-311++G** level. The π -bond rupture energies were determined by optimizing models in which the relative orientation of the R_2N and BR'_2 fragments was fixed in such a manner that the lone-pair atomic orbital on N was orthogonal to the vacant 2p-orbital on the B atom. Similar calculations were carried out on the (3c,2e) dative π -bonding systems of bisborylamines, $RN(BR'_2)_2$; the (3c,4e) π -system of bisaminoboranes, $RB(NR'_2)_2$; the trigonal (4c,2e) π -bonding systems of trisborylamines, $N(BR_2)_3$, and the (4c,6e) π -systems of trisaminoboranes, $B(NR_2)_3$. The structures of $HN(BMe_2)_2$, $MeN(BMe_2)_2$, and $MeB(NMe_2)_2$ determined by gas electron diffraction were in good agreement with those determined by calculations. The mean N–B π -bond rupture energies, $\langle D_\pi \rangle$, in the prototypical compounds H_2NBH_2 , $HN(BH_2)_2$, $HB(NH_2)_2$, $N(BH_2)_3$, and $B(NH_2)_3$ were found to depend not on the number of π -electrons, but on the number of centers. The mean π -bond rupture energies of the prototypical 2c, 3c, and 4c compounds were found to vary in the order 4.0:3.0:2.0. When H atoms at an acceptor atom (B) are replaced by more electron releasing methyl groups, $\langle D_\pi \rangle$ is significantly reduced due to a synergetic combination of destabilizing inductive effects and steric strain. When H atoms at the donor atom (N) are replaced by Me groups, the effect on $\langle D_\pi \rangle$ is determined by the balance of stabilizing inductive and destabilizing steric effects. The N–B bond distances in the 14 molecules tend to decrease with increasing mean π -bond rupture energy. Linear correlation analysis yields $R(N-B) = 149.3 \text{ pm} - (0.075 \text{ pm mol kJ}^{-1}) \langle D_\pi \rangle$ and a correlation coefficient of $\rho = 0.97$.

Introduction

The results reported in this article have been obtained in an ongoing project for the determination of the molecular structures of boron–nitrogen compounds in the gas phase.^{1,2} In our reports we have defined a N–B bond as covalent if the homolytic bond rupture energy is lower than the heterolytic, and as dative if the heterolytic bond rupture energy is lower than the homolytic.³ Minimum-energy rupture of the covalent bond in ethane yields two methyl radicals. In sharp contrast,

minimum-energy rupture of the N–B bond in the iso-electronic molecule amine-borane yields the closed shell species NH_3 and BH_3 ; the N–B σ -bond has heterolyzed and is thus dative according to our definition.

The simplest compound displaying two-center, two-electron (2c,2e) dative π -bonding between a N and a B atom is aminoborane, H_2NBH_2 .³ This molecule is iso-electronic with ethene and is therefore expected to have a similar structure. Indeed, a microwave study has shown that H_2NBH_2 has a planar structure of C_{2v} symmetry and yielded a N–B bond distance of 139.1(2) pm.⁴ Both molecules are stabilized through π -bonding.³ When the π -bond in ethene is broken by rotating one of the methylene groups 90° about the C–C axis, the

* Corresponding authors. Phone: +(47) 22 85 54 07. Fax: +(47) 22 85 54 41. E-mail: ahaaland@kjemi.uio.no; greteg@kjemi.uio.no.

(1) Østby, K.-A.; Gundersen, G. *J. Mol. Struct.* **2004**, *691*, 1, and references therein.

(2) Østby, K.-A.; Gundersen, G.; Haaland, A.; Nöth, H. *Dalton Trans.* **2005**, 2284.

(3) Haaland, A. *Angew. Chem., Int. Ed. Engl.* **1989**, *28*, 992.

(4) Sugui, M.; Takeo, H.; Matsumura, C. *J. Mol. Spectrosc.* **1987**, *123*, 286.

former π -bonding electrons are found to occupy two $p\pi$ atomic orbitals, one on each C atom. If, however, the H_2N fragment in aminoborane is rotated into an orthogonal orientation, both the former π -electrons are found to occupy an atomic orbital on the N atom; the N–B π -bond has heterolyzed and is thus dative by our definition.

The molecular structures of two methyl-substituted aminoboranes have been determined experimentally: A study of Me_2NBMe_2 by low-temperature (110 K) single-crystal X-ray crystallography (XR) has shown that the B, the N, and the four C atoms are coplanar and yielded a N–B bond distance of 140.3(1) pm,⁵ and a gas electron diffraction (GED) study of MeHNBMe_2 has yielded a B–N bond distance of 139.7(2) pm.⁶

A microwave study of the simplest bisaminoborane, $\text{HB}(\text{NH}_2)_2$, has shown that this molecule too is planar with C_{2v} symmetry.⁷ The planarity of the molecule in conjunction with the short N–B bond distances suggests that the electron lone pairs of both N atoms are delocalized over the NBN frame, resulting in a 3c,4e π -bonding system. Studies of methyl-substituted derivatives such as $\text{MeB}(\text{NMe}_2)_2$, by low-temperature XR,⁸ and more recently $\text{HB}(\text{NMe}_2)_2$ by GED and DFT calculations⁹ have yielded similar structures, except that the two dimethylamino groups in each compound are twisted in an disrotatory manner out of the N_2B plane, the twist angles varying from about 10° to about 30°. A low-temperature X-ray study of $\text{MeB}(\text{NHMe})_2$ yielded much smaller twist angles of about 5°;⁸ the magnitude of the twist may, however, be influenced by a network of intermolecular hydrogen bonds in the crystalline phase.⁸ An early GED study of the same compound yielded twist angles of about 17°,⁶ while more recent refinements have yielded twist angles that are not significantly different from zero.¹⁰

We have found no reference to the preparation of trisaminoborane $\text{B}(\text{NH}_2)_3$ in the literature. Ab initio calculations with a standard 6-31G* basis and correlation energies obtained by the CIPSI algorithm indicate that the structure of the molecule is nearly planar, but a slight pyramidality of the N atoms lowers the symmetry from D_{3h} to C_s .¹¹ Recently published DFT calculations at the B3LYP/6-311+G(2df,p) level, on the other hand, indicate a planar D_{3h} structure.¹² The planar—or near planar—equilibrium structures obtained by these calculations suggest the presence of a trigonal 4c,6e π -bonding system. The permethylated trisaminoborane, $\text{B}(\text{NMe}_2)_3$, is known and has been the subject of an accurate structure determination by low-temperature X-ray crystallography.¹³ The molecules occupy nonsymmetric sites, but the coordination geometries of the B and the three N atoms are all very close to planar. A molecular model of D_{3h} symmetry would provide optimal

conditions for the 4c,6e π -bonding system, but the three dimethylamino groups are rotated out of the BN_3 plane with twist angles varying from 28° to 35°. Except for the difference between the twist angles, the molecular symmetry is close to D_3 . The gas-phase structure of $\text{B}(\text{NHMe})_3$, determined by GED, has D_3 symmetry with twist angles of about 13°.⁶

Replacement of the central B atom in bisaminoborane by a N atom, and replacement of the two N by B atoms, leads to the formation of bisborylamine, $\text{HN}(\text{BH}_2)_2$. While bisaminoborane presents a simple molecule with a delocalized 3c,4e dative π -bonding systems, bisborylamine, $\text{HN}(\text{BH}_2)_2$, and its derivatives are expected to display 3c,2e π -bonding. We have found no reference to the synthesis of bisborylamine in the literature. Methylated derivatives are known, but to the best of our knowledge no simple bisborylamine structure has been published until now.

The structure of a simple trisborylamine, $\text{N}(\text{BR}_2)_3$, would provide an interesting example of a similar trigonal 4c,2e π -system, but no such structure seems to be available. We can find no reference to the syntheses of $\text{N}(\text{BH}_2)_3$ in the literature. Structure optimizations at the HF/6-31G* and MP2/6-31G* levels indicate that the equilibrium structure would have D_{3h} symmetry.¹⁴ $\text{N}(\text{BMe}_2)_3$ has been prepared,¹⁵ but the structure has not been determined.

In the present article we report (i) DFT (B3PW91/6-311++G**) optimized structures of the 2c,2e dative π -bonded systems $\text{R}_2\text{NBR}'_2$ (R, R' = H or Me); (ii) DFT-optimized structures of the 4c,6e π -systems $\text{B}(\text{NR}_2)_3$ and of the 4c,2e π -systems $\text{N}(\text{BR}_2)_3$, R = H or Me; (iii) DFT-optimized structures of the prototypical 3c,4e and 3c,2e π -bonding systems $\text{HB}(\text{NH}_2)_2$ and $\text{HN}(\text{BH}_2)_2$ respectively; (iv) the molecular structure of the 3c,4e π -bonded bisaminoborane $\text{MeB}(\text{NMe}_2)_2$ determined by GED and DFT calculations to complement our earlier study⁹ of $\text{HB}(\text{NMe}_2)_2$; (v) the molecular structures of two bisborylamines, $\text{HN}(\text{BMe}_2)_2$ and $\text{MeN}(\text{BMe}_2)_2$, determined by GED and DFT structure optimizations; these are, to the best of our knowledge, the first simple boron–nitrogen compounds with 3c,2e π -bonding systems to be characterized structurally; and (vi) a discussion of N–B bond distances and π -bond rupture energies in all these molecules.

Results and Discussion

Dative π -Bonding in Aminoboranes. Structure optimizations of H_2NBH_2 , Me_2NBH_2 , and H_2NBMe_2 by DFT calculations at the B3PW91/6-311++G** level yield equilibrium structures of C_{2v} symmetry, which implies that all atoms, with the exception of some methyl group hydrogen atoms, are coplanar. The orientation of the methyl groups in Me_2NBH_2 or H_2NBMe_2 is such that one C–H bond in each group is syn positioned relative to the N–B bond; $\tau(\text{HCNB})$ or $\tau(\text{HCBN}) = 0^\circ$. Structure optimization of Me_2NBMe_2 yields an equilibrium structure where the C_2NBC_2 frame has near C_{2v} symmetry, but—presumably due to steric repulsion between H atoms—one of the methyl groups bonded to B has been rotated into an anti

(5) Boese, R.; Niederprüm, N.; Bläser, D. *Struct. Chem.* **1992**, *3*, 399.

(6) Almenningen, A.; Gundersen, G.; Mangerud, M.; Seip, R. *Acta Chem. Scand.* **1981**, *A 35*, 341.

(7) Thorne, L. R.; Gwinn, W. D. *J. Am. Chem. Soc.* **1982**, *104*, 3822.

(8) Niederprüm, N.; Boese, R.; Schmid, G. *Z. Naturforsch.* **1991**, *46b*, 84.

(9) Østby, K.-A.; Fjeldberg, T.; Gundersen, G. *J. Mol. Struct.* **2001**, *567–568*, 247.

(10) Østby, K.-A.; Gundersen, G. Unpublished results.

(11) Volatron, F.; Demachy, I. *Chem. Phys. Lett.* **1992**, *198*, 253.

(12) Kormos, B. L.; Cramer, C. J. *Inorg. Chem.* **2003**, *42*, 6691.

(13) Schmid, G.; Boese, R.; Bläser, D. *Z. Naturforsch.* **1982**, *37b*, 1230.

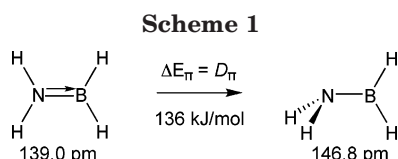
(14) Skancke, A. *J. Phys. Chem.* **1994**, *98*, 5234.

(15) Storch, W.; Nöth, H. *Chem. Ber.* **1977**, *110*, 1636.

Table 1. Molecular Structures of Aminoboranes, $R_2NBR'_2$ ($R, R' = H$ or Me)^a

	H_2NBH_2		Me_2NBH_2	H_2NBMe_2	Me_2NBMe_2	
	DFT	MW ^b	DFT	DFT	DFT	XR ^c
Equilibrium Structures						
symmetry	C_{2v}	C_{2v}	C_{2v}	C_{2v}	C_s	C_s
bond distances (pm)	r_e	r_0	r_e	r_e	r_e	r
N–B	139.0	139.1(2)	138.9	140.3	141.1	140.3(1)
B–(H/C)	119.6	119.5(4)	119.7	158.1	158.8	158.4 ^d
N–(H/C)	100.8	100.4(2)	145.3	100.8	145.2	145.7 ^d
⟨C–H⟩			109.5	109.6	109.7	
Valence Angles (deg)						
N–B–(H/C)	118.9	118.9(1)	119.0	119.5	121.4	121.1 ^d
B–N–(H/C)	123.3	122.9(1)	123.3	123.2	124.4	124.6 ^d
⟨B–C–H⟩				111.9	112.1	
⟨N–C–H⟩			110.5		110.9	
Orthogonal Forms						
symmetry	C_s		C_s	C_s	C_s	
$\Delta E_\pi = D_\pi$ (kJ mol ⁻¹)	136		146	114	107	
N–B bond distance	146.8		146.2	148.6	148.6	

^a Bond distances and valence angles in the equilibrium structures obtained by DFT optimizations, of H_2NBH_2 by MW spectroscopy, and of Me_2NBMe_2 by low-temperature X-ray diffraction. Relative energies and N–B bond distances in the transition states for internal rotation obtained by DFT optimizations of orthogonal models. ^b Reference 4. ^c Reference 6. ^d Average values.



orientation. The molecular symmetry is thus reduced to C_s . Bond distances and valence angles of the four compounds are listed in Table 1.^{16,19} Before proceeding we pause to note that the equilibrium structure parameters of H_2NBH_2 obtained by DFT calculations are in excellent agreement with the (r_0) parameters obtained by MW spectroscopy⁴ and that the optimized structure of Me_2NBMe_2 (including the orientations of the methyl groups) is in good agreement with those obtained in a low-temperature (110 K) X-ray study.⁵ See Table 1.

The trigonal planar coordination geometries of both N and B atoms in each compound indicate that the covalent σ -bond between them is overlaid by a dative π -bond. The dative π -bond in H_2NBH_2 was then broken by rotating the amino group through 90° into an orientation where the H_2N plane is orthogonal to the BH_2 plane, and the p-orbital on the N atom containing the electron lone pair is orthogonal to the vacant p-orbital on the B atom. When structure optimization was continued under C_s symmetry, the B–N bond distance increased from 139.0 to 146.8 pm and the N atom became pyramidal. We refer to the energy difference between the optimized planar and orthogonal forms as the dative π -bond rupture energy, D_π . Similar optimizations of the orthogonal forms of Me_2NBH_2 , H_2NBMe_2 , and Me_2NBMe_2 yielded the N–B bond distances and the π -bond rupture energies listed in Table 1.^{18,19} The optimized orthogonal forms are characterized by one imaginary vibrational frequency and represent

the transition states for internal rotation about the N–B bonds. The calculated π -bond rupture energy in Me_2NBMe_2 (107 kJ mol⁻¹) is in fact in good agreement with the barrier to internal rotation in $Me_2NBMePh$, Ph = phenyl, determined by variable-temperature NMR spectroscopy, viz., 110.0 kJ mol⁻¹.²⁰

We now proceed to compare the strength of the dative π -bonds in aminoboranes to the strength of the dative σ -bonds in amine-boranes, $R_3NBR'_3$ ($R, R' = H$ or Me).

(i) The energy required to break the dative π -bond in H_2NBH_2 is calculated to be 136 kJ mol⁻¹, while the best experimental estimate of the dissociation energy of H_3NBH_3 is 130 ± 4 kJ mol⁻¹;³ it appears that the strength of the prototypical dative N–B π -bond is very similar to the strength of the prototypical dative σ -bond. Both are much weaker than a covalent N–B σ -bond: the energy of a covalent bond estimated from the energies of formation of the cubic and hexagonal forms of crystalline boron nitride is 368 ± 8 kJ mol⁻¹.³

(ii) The strength of the dative σ -bond in amine-boranes is very sensitive to the inductive effects of substituents, particularly those at the acceptor atom. Thus replacement of the three H atoms bonded to the B atom in H_3NBH_3 by more electron releasing methyl groups to form H_3NBMe_3 reduces the dissociation energy by about 55% from 130 ± 4 to 58 ± 1 kJ mol⁻¹, while replacement of the three H atoms bonded to the donor atom (N) increases the dissociation energy by about 12% to 145 ± 2 kJ mol⁻¹.³ Inspection of the data in Table 1 shows that replacement of the two H atoms bonded to the B atom in H_2NBH_2 by Me groups reduces the π -bond rupture energy by about 22 kJ mol⁻¹, or 16%, while replacement of the two H atoms bonded to N increases the bond strength of the dative π -bond by about 10 kJ mol⁻¹, or 7%. It appears that dative π -bonds are significantly less sensitive than dative σ -bonds to the inductive effects of σ -bonded substituents.

(iii) The inductive effects on the strength of the dative σ -bond in amine-borane complexes appear to be additive; replacement of the three H atoms bonded to the N atom in H_3NBH_3 or H_3NBMe_3 by methyl groups increases the strength of the dative σ -bond in the former

(16) For the equilibrium structures of H_2NBH_2 and Me_2NBMe_2 optimized at the B3LYP/6-31G* level see: Gilbert, T. M. *Organometallics* **1998**, *17*, 5513.

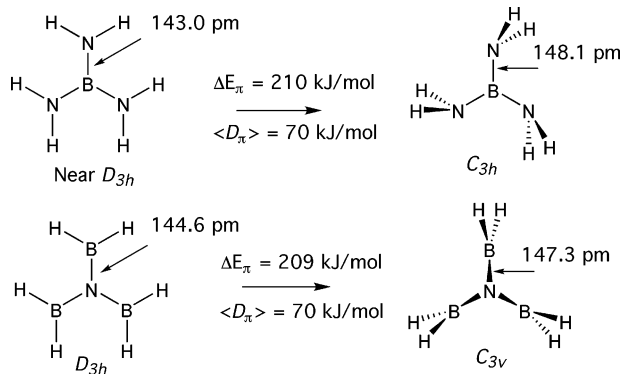
(17) For the equilibrium structures of H_2NBH_2 and H_2NBMe_2 optimized at the MP2/6-31+G(d) level see: Poon, C.; Mayer, P. M. *Can. J. Chem.* **2002**, *80*, 25.

(18) For the structures and relative energies of planar and orthogonal H_2NBH_2 optimized at the HF/6-311+G** level see: Mo, Y.; Peyerimhoff, S. D. *Theor. Chem. Acc.* **1999**, *101*, 311.

(19) For the structures and relative energies of planar and orthogonal H_2NBH_2 optimized at the B3LYP/6-311+G(2df,p) level see ref 12.

(20) Totani, T.; Tori, J.; Murakami, J.; Watanabe, H. *Org. Magn. Reson.* **1971**, *3*, 627.

Scheme 2



by about 15 kJ mol⁻¹ and in the latter by about 16 kJ mol⁻¹.³ Similarly the replacement of the two H atoms on the N atom in H₂NBH₂ by methyl groups increases the strength of the dative π -bond by 10 kJ mol⁻¹, while—in sharp contrast—the replacement of the two H atoms in H₂NBMe₂ by methyl groups *decreases* the calculated dative π -bond energy by 7 kJ mol⁻¹. This destabilizing effect must—at least in part—be due to steric repulsion between Me groups in Me₂NBMe₂; the distance between C atoms in cis positions is only 307 pm as compared to a methyl group van der Waals diameter of 400 pm.²¹

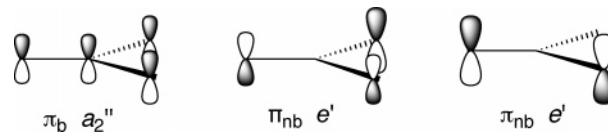
The upshot is that the dative π -bonds in the two compounds where the B atom is bonded to methyl groups are much weaker than the π -bonds in the two molecules where it is bonded to H atoms, and inspection of Table 1 shows that the calculated equilibrium B–N bond distances are about 2.0 pm longer in the two aminoboranes with the weaker π -bonds, viz., H₂NBMe₂ and Me₂NBMe₂.

Dative π -Bonding in Trisaminoboranes and Trisborylamines. Structure optimizations of N(BH₂)₃ by DFT calculations yielded the planar D_{3h} equilibrium structure shown in Scheme 2. Optimization of B(NH₂)₃ under D_{3h} symmetry, on the other hand, yielded a model characterized by one imaginary vibrational frequency. Continued optimization under D_3 symmetry led to an equilibrium structure where all NH₂ groups had been rotated about 6° out of the BN₃ plane. The energy of this equilibrium structure was, however, only 0.03 kJ mol⁻¹ below the optimal D_{3h} model.²² We shall therefore base our discussion on the more symmetric model. The planar D_{3h} structures are, of course, optimal for the establishment of strong four-center π -bonding systems.

The DFT calculations indicate that the highest occupied molecular orbital (HOMO) of N(BH₂)₃ is the 4c π -bonding orbital of a_2'' symmetry (π_b) shown in Scheme 3. Trisaminoborane has four electrons more than trisborylamine; these electrons are found to occupy the two degenerate, nonbonding, N-centered, π -orbitals of e' symmetry (π_{nb}). The next orbital in order of decreasing energy was the π_b . See Scheme 3.

When the π -bonding system in B(NH₂)₃ was broken by rotating the three H₂N groups into orthogonal orientations and structure optimization continued under

Scheme 3



C_{3h} symmetry, the B–N bond distances increased by 5 pm and the N atoms became pyramidal.²² See Scheme 2. In the following we refer to the energy difference between the optimized orthogonal form and the planar equilibrium structure $\Delta E_\pi = 210$ kJ mol⁻¹ as the total π -bonding energy and to a third of this energy as the mean N–B π -bond rupture energy $\langle D_\pi \rangle = \Delta E_\pi/3 = 70$ kJ mol⁻¹. The optimized orthogonal form corresponds to the transition state for concerted internal rotation of the amino groups. It is characterized by three imaginary vibrational frequencies, which shows that both concerted and nonconcerted internal rotation lead to a drop in energy.

When the boryl groups in N(BH₂)₃ were rotated into orthogonal orientations and the optimization was continued under C_{3v} symmetry in order to determine the total π -bond energy, the central N atom became pyramidal (\angle BNB = 101.3°) and the N–B bond distance increased by about 3 pm. Again the optimized structure was characterized by three imaginary frequencies corresponding to internal rotation of the ligands.

Nearly 25 years ago one of us published the results of a comparative computational study of B(NH₂)₃ and N(BH₂)₃ at the HF level with DZ basis sets and polarization functions at the B and N atoms.²³ Partial structure optimizations yielded equilibrium structures of D_{3h} symmetry. Mulliken population analysis indicated that the π -character of the N–B bonds in the two compounds was equal, and the calculated barrier to rigid internal rotation of *one* NH₂ ligand in B(NH₂)₃ was essentially equal to the barrier to rigid rotation of a BH₂ ligand in N(BH₂)₃. In the present study we find that the total π -bond energy of trisborylamine, $\Delta E_\pi = 209$ kJ mol⁻¹, is indistinguishable from that of the trisaminoborane. Is there any reason to expect that a trigonal arrangement of three π -donor atoms around a π -acceptor or the arrangement of three π -acceptor atoms around a π -donor should lead to the formation of two equally strong π -bonding systems? Since simple Hückel calculations are known to bring out the consequences of connectivity and symmetry, we turned to such calculations for guidance.²⁴

The results of such calculations are summarized in Figure 1. In the orthogonal form of B(NH₂)₃ the three

(23) Gundersen, G. *Acta Chem. Scand.* **1981**, A 35, 729.

(24) We first consider trisaminoborane. Denoting the central B atom as number 1 and numbering the three N atoms from 2 to 4, denoting the Coulomb integrals by α_B and α_N , the resonance integral as β , and neglecting overlap integrals, one obtains the following secular equations: $(\alpha_B - \epsilon)c_1 + \beta c_2 + \beta c_3 + \beta c_4 = 0$, $\beta c_1 + (\alpha_N - \epsilon)c_2 + 0 + 0 = 0$, $\beta c_1 + 0 + (\alpha_N - \epsilon)c_3 + 0 = 0$, $\beta c_1 + 0 + 0 + (\alpha_N - \epsilon)c_4 = 0$. Setting the secular determinant equal to zero one obtains a fourth-degree equation for the orbital energy ϵ . The roots are $\epsilon_1 = \epsilon_b = (1/2)\{(\alpha_B + \alpha_N) - \sqrt{[(\alpha_B - \alpha_N)^2 + 4C_n\beta^2]}\}$, $\epsilon_2 = \epsilon_3 = \alpha_N$, and $\epsilon_4 = \epsilon_{ab} = (1/2)\{(\alpha_B + \alpha_N) + \sqrt{[(\alpha_B - \alpha_N)^2 + 4C_n\beta^2]}\}$, where $C_n = 3$ is the coordination number of the central B atom. The first root corresponds to the a_2'' π -bonding orbital in Scheme 3, the second and third to the two degenerate e' nonbonding orbitals, and the fourth to an antibonding orbital. A similar treatment of the π -bonding system in trisborylamine yields a bonding orbital of a_2'' symmetry with energy equal to $\epsilon_b = \epsilon_1$ above, two nonbonding orbitals with energy equal to α_B , and an antibonding orbital with energy equal to ϵ_4 .

(21) Bondi, A. *J. Chem. Phys.* **1964**, 68, 441.

(22) For the structures and relative energies of the planar and orthogonal forms of B(NH₂)₃ optimized at the B3LYP/6-311+G(2df,p) level see ref 12. This article also describes a second, less stable, orthogonal form obtained from the C_{3h} model shown in Scheme 2 by rotating one of the amino groups 180° about the N–B bond.

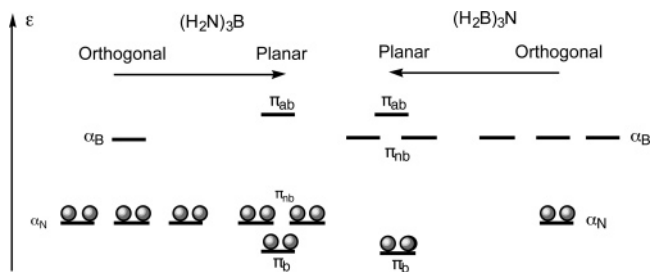


Figure 1. Schematic representation of the four-center π -bonding systems of $\text{B}(\text{NH}_2)_3$ and $\text{N}(\text{BH}_2)_3$ as described by Hückel calculations. From left to center page: Occupied MOs in orthogonal and planar forms of trisaminoborane. From right to center page: Occupied MOs in orthogonal and planar forms of trisborylamine. Note that the two orbitals marked π_b have the same energy.

electron lone pairs occupy nonbonding atomic orbitals localized on the three N atoms. In the planar form one electron pair occupies the bonding a_2'' π -orbital, and the remaining two occupy delocalized, nonbonding e' orbitals of (approximately) unaltered energy. Within the framework of the Hückel method the total π -bonding energy is equal to the difference $\Delta E_\pi = 2\alpha_N - 2\epsilon_b$, where α_N is the energy of a lone-pair orbital on N and ϵ_b the energy of the π_b -orbital. In the orthogonal form of $\text{N}(\text{BH}_2)_3$ the electron lone pair occupies an atomic orbital on the central N atom. In the planar form it occupies a four-center a_2'' π -bonding orbital of the same energy as in the trisaminoborane and the total π -bonding energy is again $\Delta E_\pi = 2\alpha_N - 2\epsilon_b$. Given the highly approximate nature of Hückel calculations, the close agreement between the π -bonding energies of trisaminoborane and trisborylamine obtained by the DFT calculations is certainly to a large degree fortuitous, but in the following we shall accept the conclusion that the arrangement of three acceptor atoms around a donor and of three donor atoms around an acceptor are equally favorable for dative π -bonding. Where different total π -bond energies are encountered, we shall look for explanations in terms of the inductive effects of substituents. Analysis of the 4c π -bonding orbitals indicates that the negative charge transferred to the central B atom in $\text{B}(\text{NH}_2)_3$ is three times larger than the negative charge transferred from the central N atom to each of the three B atoms in $\text{N}(\text{BH}_2)_3$: the amounts of charge transferred from π -donor to π -acceptor atoms in the two molecules are equal.

Even though the total π -bonding energies of the two compounds are equal, the N–B bond distance in $\text{N}(\text{BH}_2)_3$ is 1.6 pm greater than in $\text{B}(\text{NH}_2)_3$, perhaps because the covalent σ -bond is weaker.²³

Before going on to describe the structures of methylated derivatives we pause to note that while the total π -bonding energies ΔE_π of trisaminoborane and trisborylamine are about 50% higher than in aminoborane H_2NBH_2 , the mean π -bond rupture energies $\langle D_\pi \rangle$ in trisaminoborane and trisborylamine are about 50% smaller than in H_2NBH_2 .

Structure optimization of the methyl-substituted compounds $\text{B}(\text{NMe}_2)_3$ and $\text{N}(\text{BMe}_2)_3$ yielded equilibrium structures of D_3 rather than D_{3h} symmetry. The coordination geometries of both B or N atoms remain strictly planar, but the dimethylamino groups in the former and the dimethylboryl groups in the latter are rotated some

Table 2. Molecular Structures of Tris(dimethylamino)borane and Tris(dimethylboryl)amine^a

	$\text{B}(\text{NMe}_2)_3$		$\text{N}(\text{BMe}_2)_3$
	DFT ^b	XR ^c	DFT
Equilibrium Structures			
symmetry	D_3		D_3
bond distances (pm)	r_e	r	r_e
N–B	144.3	143.9(1)	146.3
(N/B)–C	144.5	145.3(1)	157.9
$\langle \text{C–H} \rangle$	109.7		109.6
Valence Angles (deg)			
B–N–C/N–B–C	123.4	123.9(1)	121.5
$\langle (\text{N/B})\text{–C–H} \rangle$	111.2		111.8
Dihedral Angles (deg)			
N–B–N–C/B–N–B–C	32.8	31.1	34.6
Orthogonal Forms			
symmetry	C_{3h}		C_{3v}
$\Delta E_\pi; \langle D_\pi \rangle$ (kJ mol ⁻¹)	202; 67		138; 46
N–B bond distances	148.1		148.0

^a Bond distances and valence and dihedral angles in the equilibrium structures obtained by DFT structure optimizations and in $\text{B}(\text{NMe}_2)_3$ determined by low-temperature X-ray diffraction. Relative energies of and N–B bond distances in the transition states for concerted internal rotation of NMe_2 or BMe_2 groups obtained by DFT optimizations of orthogonal models. ^b Reference 1. ^c Reference 13. Structure parameters and their estimated standard deviations have been averaged to D_3 symmetry.

32–35° out of the BN_3 or NB_3 planes. This rotation is almost certainly due to steric repulsion between methyl groups: in the equilibrium conformations the shortest distances between C atoms in different NMe_2 or BMe_2 groups are 315 and 324 pm, respectively, as compared to the accepted methyl group van der Waals diameter of 400 pm.²¹ Bond distances and valence angles are listed in Table 2. We note that the calculated structure parameters of $\text{B}(\text{NMe}_2)_3$ are in good agreement with those obtained by low-temperature X-ray diffraction.¹³

The orthogonal forms of $\text{B}(\text{NMe}_2)_3$ and $\text{N}(\text{BMe}_2)_3$, like the prototypes $\text{B}(\text{NH}_2)_3$ and $\text{N}(\text{BH}_2)_3$, have C_{3h} and C_{3v} symmetry, respectively. Total and mean π -bond energies and N–B bond distances are listed in Table 2.

The out-of-plane rotations of the NMe_2 or BMe_2 groups are expected to weaken the dative π -bonding in the equilibrium structures. The overlap integrals between $p\pi$ -orbitals on neighboring N and B atoms will be reduced by a factor of $\cos \tau \approx 0.83$, and it does not seem unreasonable that the π -bonding energy will be similarly reduced. The replacement of the six H atoms in $\text{B}(\text{NH}_2)_3$ by methyl groups, on the other hand, is expected to enhance π -bonding. The total π -bonding energy of $\text{B}(\text{NMe}_2)_3$, 202 kJ mol⁻¹, is in fact close to that of $\text{B}(\text{NH}_2)_3$; it seems that the effects of reduced overlap and of more electron releasing substituents cancel one another. In $\text{N}(\text{BMe}_2)_3$, however, they are expected to act in the same direction and the π -bonding energy is indeed reduced by 34% relative to $\text{N}(\text{BH}_2)_3$.

Dative π -Bonding in Bisaminoborane and Bisborylamine. Structure optimizations of $\text{HB}(\text{NH}_2)_2$ and $\text{HN}(\text{BH}_2)_2$ yielded planar equilibrium structures of C_{2v} symmetry. See Scheme 4. Note that H atoms characterized by dihedral angles $\tau(\text{N–B–N–H})$ or $\tau(\text{B–N–B–H}) = 0^\circ$ are denoted by a *c* (for cis) and that those characterized by dihedral angles equal to 180° are denoted by a *t* (for trans). Bond distances and valence angles are listed in Table 3.²⁵ The calculated structure of the bisaminoborane is seen to be in excellent agreement with the results of a microwave study.⁷ Rotation

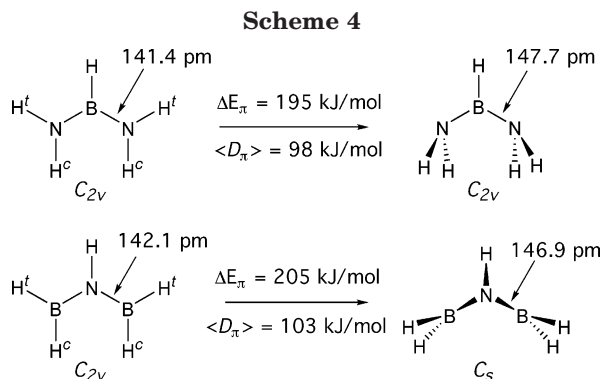


Table 3. Molecular Structures of Bis(dimethylamino)borane and Bis(dimethylboryl)amine^a

	HB(NH ₂) ₂		HN(BH ₂) ₂	
	DFT	MW ^b		DFT
Equilibrium Structures				
symmetry	<i>C</i> _{2v}	<i>C</i> _{2v}		<i>C</i> _{2v}
bond distances (pm)	<i>r</i> _e	<i>r</i> ₀	<i>r</i> _e	<i>r</i> _e
N–B	141.4	141.8(1)	N–B	142.1
B–H	119.8	119.3(1)	N–H	101.3
N–H ^t	100.5	100.0(5)	B–H ^t	119.6
N–H ^c	100.7	100.0(3)	B–H ^c	119.3
Valence Angles (deg)				
N–B–N	123.0	122.0(3)	B–N–B	126.0
B–N–H ^t	121.8	121.1(1)	N–B–H ^t	119.3
B–N–H ^c	124.5	123.7(6)	N–B–H ^c	118.7
Orthogonal Forms				
symmetry	<i>C</i> _{2v}			<i>C</i> _s
Δ <i>E</i> _π ; < <i>D</i> _π > (kJ mol ⁻¹)	195; 97			205; 103
N–B bond distances	147.7			146.9

^a Bond distances and valence and dihedral angles in the equilibrium structures obtained by DFT structure optimizations and in HB(NH₂)₂ determined by microwave spectroscopy. Relative energies of and N–B bond distances in the transition states for concerted internal rotation of NH₂ or BH₂ groups obtained by DFT optimizations of orthogonal models. ^b Reference 7.

of the two amine groups in HB(NH₂)₂ into orthogonal orientations and continued optimization, still under *C*_{2v} symmetry, led to a stationary structure characterized by two imaginary NH₂ rotation modes that corresponds the transition point for concerted internal rotation of the amino groups.²⁵ See Scheme 4.

Rotation of the two boryl groups in HN(BH₂)₂ into orthogonal orientations and continued optimization under *C*_{2v} symmetry led to a stationary structure characterized by *three* imaginary modes, two BH₂ rotation modes and a nitrogen pyramidalization mode. Pyramidalization of the N atom reduces the molecular symmetry to *C*_s, and continued optimization under this symmetry converges to the planar *C*_{2v} equilibrium structure. The total π -bonding energy of this compound was therefore estimated by assuming that the direction of the electron lone pair on the N atom is indicated by a vector *lp* making equal angles with the three bonds radiating from it. Continued optimization under *C*_s symmetry, but with the planar boryl groups fixed in orientations that rendered the two B–H bonds and the *lp* vector coplanar, converged to a model with a distinctly pyramidal N atom and a BNB valence angle of

(25) For the structures and relative energies of the planar and orthogonal form of HB(NH₂)₂ optimized at the B3LYP/6-311+G(2df,p) level see ref 12. This article also describes a second, slightly less stable, orthogonal form obtained from the *C*_{2v} model shown in Scheme 4 by rotating both amino groups 180° about the N–B bond.

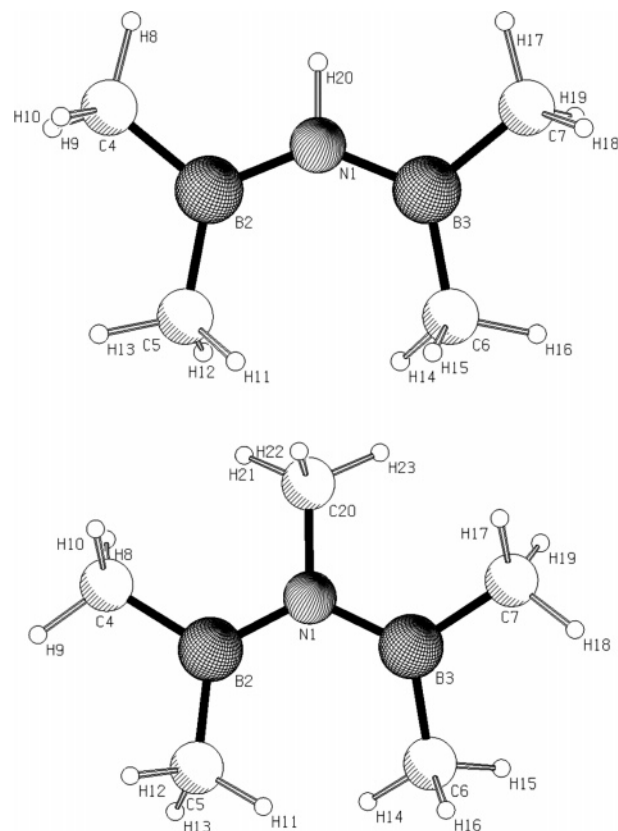


Figure 2. Optimized structures and numbering of the atoms in HN(BMe₂)₂ (above) and MeN(BMe₂)₂ (below). The C atoms in HB(NMe₂)₂ and MeB(NMe₂)₂ are numbered in the same manner. In the text and tables we refer to carbon atoms 4 and 7 in each of the four compounds as trans, C^t, and 5 and 6 as cis, C^c, and to the carbon atom bonded to the central N or B atom in MeN(BMe₂)₂ or MeB(NMe₂)₂, respectively, as C*. Program Pluton.²⁷

112.9°. The total π -bonding energy estimated in this manner is indicated in Scheme 4.

Hückel calculations on the equilibrium structures lead to results similar to those obtained by calculations on N(BH₂)₃ and B(NH₂)₃. The π -electron pair in HN(BH₂)₂ is found to occupy a 3c bonding orbital of b₁ symmetry. One of the two π -electron pairs in HB(NH₂)₂ is found to occupy a similar b₁ bonding orbital of the same energy, while the other occupies a nonbonding orbital of a₂ symmetry. Thus Hückel calculations indicate that the two molecules should be equally stabilized by dative π -bonding. An early comparative computational study of the two compounds at the HF/DZ+P level also yielded essentially equal total π -bonding energies for the two compounds.²⁶ In the present study the total π -bond energies of the two systems are found to differ by 6%.

The mean π -bond rupture energies in the simplest 2c system H₂NBH₂, in the two simplest 3c systems HB(NH₂)₂ and HN(BH₂)₂, and in the simplest 4c systems B(NH₂)₃ and N(BH₂)₃ are seen to vary in the order 136 kJ mol⁻¹:101 kJ mol⁻¹:70 kJ mol⁻¹ or about 4.0:3.0:2.0.

Molecular Structures and Dative π -Bonding in Methyl-Substituted Bisaminoboranes and Bisborylamines by DFT Calculations and Gas Electron Diffraction. Structure optimization of bis(dimethylbo-

(26) Fjeldberg, T.; Gundersen, G.; Jonvik, T.; Seip, H. M.; Sæbø, S. *Acta Chem. Scand.* **1980**, A 34, 547.

Table 4. Molecular Structures of HB(NMe₂)₂, MeB(NMe₂)₂, HN(BMe₂)₂, and MeN(BMe₂)₂ Obtained by DFT Structure Optimizations and GED Structure Refinements^a

	HB(NMe ₂) ₂ ^b		MeB(NMe ₂) ₂		HN(BMe ₂) ₂		MeN(BMe ₂) ₂	
	DFT	GED	DFT	GED	DFT	GED	DFT	GED
Equilibrium Structures					Equilibrium Structures			
symmetry	C ₂	C ₂	C ₁	C ₁	symmetry	C ₂	C ₂	C ₁
distances (pm)	r _e	r _a	r _e	r _a	distances (pm)	r _e	r _a	r _e
B–N(2/3)	142.1	142.5(4)	143.7/143.5	143.6/143.4(3)	N–B(2/3)	143.7	143.7(2)	144.6/144.7
N(2/3)–C ^t	144.9	145.6(2)	144.8/144.8	145.5/145.5(2)	B(2/3)–C ^t	158.0	158.2(2)	158.7/158.5
N(2/3)–C ^c	144.7	145.4(2)	144.9/144.8	145.6/145.5(2)	B(2/3)–C ^c	157.8	158.1(2)	158.0/158.0
B–(H/C)	120.1	[121.7]	159.2	159.7(4)	N–H/C	102.5	[102.5]	147.4
⟨C–H⟩	109.6	110.6(2)	109.6	110.7(1)	⟨C–H⟩	109.6	110.6(1)	109.5
C ^c ...C ^c	321	321(1)	307	307(1)	C ^c ...C ^c	324	330(1)	311
C ^t ...C [*]			310/301	307/300(1)	C ^t ...C [*]			291
Valence Angles (deg)	∠ _e	∠ _a	∠ _e	∠ _a	Valence Angles (deg)	∠ _e	∠ _a	∠ _e
NBN	127.9	127.8(5)	120.6	121.2(4)	B–N–B	135.2	136.2(5)	126.5
B–N(2/3) ^t	120.1	119.9(3)	123.8/122.8	123.4/122.4(3)	N–B(2/3)–C ^t	118.0	117.9(2)	119.8/120.1
B–N(2/3)–C ^c	127.1	127.3(2)	124.1/124.8	124.5/125.2(3)	N–B(2/3)–C ^c	123.0	123.4(3)	123.9/123.7
C ^t –N(2/3)–C ^c	112.8	112.7(3)	111.6/111.9	111.6/111.9(3)	C ^t –B(2/3)–C ^c	119.0	118.7(4)	116.3/116.2
N(2/3)–B–(H/C)	116.1	116.1(2)	120.7/118.7	120.4/118.9(2)	B(2/3)–N–(H/C)	112.4	111.9(2)	116.8/116.6
⟨ACH⟩ ^a	111.1	111.4(2)	111.4	110.6(2)	⟨ACH⟩ ^a	111.8	112.0(2)	111.0
Dihedral Angles (deg)	τ _e	τ _a	τ _e	τ _a	Dihedral Angles (deg)	τ _e	τ _a	τ _e
N(3)–B–N(2)–C ^c	15.9	14.7(15)	28.8	27.5(6)	B(3)–N–B(2)–C ^c	0.9	[0.9]	10.8
N(2)–B–N(3)–C ^c			25.5	24.2(6)	B(2)–N–B(3)–C ^c			22.0
N(3)–B–N(2)–C ^t	–166.0	–167.6(12)	–159.3	–160.6(6)	B(3)–N–B(2)–C ^t	–178.9	[–178.9]	–172.8
N(2)–B–N(3)–C ^t			–163.2	–164.5(6)	B(2)–N–B(3)–C ^t			–162.0
Orthogonal Forms					Orthogonal Forms			
symmetry	C _{2v}		C _s		symmetry	C _s		C _s
ΔE _π ; ⟨D _π ⟩ (kJ mol ^{–1})	183; 91		163; 81		ΔE _π ; ⟨D _π ⟩ (kJ mol ^{–1})	165; 82		143; 72
N–B (pm)	146.5		148.1		N–B (pm)	148.3		148.0

^a Relative energies of and N–B bond distances obtained by DFT optimization of orthogonal models. Estimated standard deviations in parentheses in units of the last digit. Nonrefined parameters in square brackets. *c* = cis, *t* = trans. A = B or N. ^b Reference 9.

ryl)amine, HN(BMe₂)₂, leads to an equilibrium structure of C₂ symmetry. A ball-and-stick model is shown in Figure 2, and the most important structure parameters are listed in Table 4. C₂ symmetry implies that the coordination geometry of the N atom is planar. The sum of the three valence angles at each B atom, 360.0°, shows that their coordination geometries are planar too, even though this is not required by symmetry. Inspection of the structure parameters shows that the molecular symmetry is close to C_{2v}: the mirror symmetries are only destroyed by a minute (1°) rotation of the dimethylboryl groups about the N–B bonds. Least-squares structure refinements to the gas electron diffraction (GED) data were based on a model of C₂ symmetry with the BMe₂ groups fixed in the calculated orientations. See Table 6. The difference between the B–C^t and the B–C^c bond distances was fixed at the calculated value; the mean B–C bond distance was refined along with the N–B bond distance, the three valence angles ∠BNB, ∠N–B–C^t, ∠N–B–C^c, three parameters determining the position of H atoms, and eight root-mean-square vibrational amplitudes.

The calculated structure of the bisborylamine HN(BMe₂)₂ is in fact very similar to that previously obtained for the corresponding bisaminoborane HB(NMe₂)₂.⁹ Structure optimization of the latter also led to an equilibrium structure of C₂ symmetry, the coordination geometry of the central B atom is planar by symmetry, and the sum of the three valence angles at each N is equal to 360.0°. In HB(NMe₂)₂, however, the deviation from C_{2v} symmetry is significant, the dihedral angles τ(N–B–N–C^c) being 15.9°.

Table 5. Gas Electron Diffraction (GED) Data Collection and Structure Refinements

compound	HN(BMe ₂) ₂	
detector plates	KODAK ^a	
nozzle temperature/°C	15 ± 3	
nozzle-to-plate distances/cm	48	20
number of plates ^b	5	5
s _{min} ; s _{max} ; Δs/nm ^{–1}	20.00; 195.00; 1.25	80.00; 410.00; 2.50
R-factors ^b	0.026	0.055
compound	MeN(BMe ₂) ₂	
detector plates	FUJI ^c	
nozzle temperature/°C	25 ± 3	
nozzle-to-plate distances/cm	50	25
number of plates ^d	3	3
s _{min} ; s _{max} ; Δs/nm ^{–1}	20.00; 125.00; 1.25	42.50; 255.00; 2.50
R-factors ^b	0.016/0.030	0.061/0.057
compound	MeB(NMe ₂) ₂	
detector plates	KODAK ^a	
nozzle temperature/°C	37 ± 3	
nozzle-to-plate distances/cm	48	20
number of plates	6	3
s _{min} ; s _{max} ; Δs/nm ^{–1}	20.00; 195.0; 1.25	80.00; 410.00; 2.50
R-factors ^b	0.027	0.052

^a Kodak electron image plates. ^b R = √[Σw(I_{obs} – I_{cal})²/ΣwI_{obs}]. ^c FUJI imaging plates BAS-III. ^d Each plate was scanned in two different directions.

Structure optimization of the permethylated bisborylamine MeN(BMe₂)₂ led to an equilibrium structure of C₁ symmetry: a 2-fold symmetry axis is incompatible with the presence of a methyl group at the central N atom. A ball-and-stick model is shown in Figure 2, and structure parameters are listed in Table 4. Despite the

Table 6. Least-Squares Structure Refinements of HN(BMe₂)₂, Symmetry C₂.

independent parameter	constraints
Bond Distances (pm)	
N–B	
mean B–C	R(B–C ^f) – R(B–C ^c) fixed
mean C–H	all differences between C–H bonds fixed
N–H fixed	
Valence Angles (deg)	
B–N–B	
N–B–C ^f	
N–B–C ^c	
mean B–C–H	all differences between B–C–H angles fixed
Dihedral Angles (deg)	
τ (B–N–B–C ^f) and τ (B–N–B–C ^c) fixed	
N–B(2)–C(4)–H(8)	all differences between τ (N–B–C ^f –H) fixed all C ^c methyl groups in fixed orientations

Table 7. Least-Squares Structure Refinements of MeA(EMe₂)₂, Symmetry C_s^a

independent parameter	constraints
Bond Distances (pm)	
A–C*	
mean A–E	R(A–E(3)) – R(A–E(2)) fixed
mean E–C	All differences between E–C bonds fixed
mean C–H	All differences between C–H bonds fixed
Valence Angles (deg)	
E–A–E	\angle (E(3)–A–C*) – \angle (E(2)–A–C*)
mean A–E–C ^f	\angle (A–E(3)–C ^f) – \angle (A–E(2)–C ^f)
mean A–E–C ^c	\angle (A–E(3)–C ^c) – \angle (A–E(2)–C ^c)
mean (A/E)–C–H	all differences between (A/E)–C–H angles fixed for MeN(BMe ₂) ₂ all (A/E)–C–H fixed for MeB(NMe ₂) ₂
Dihedral Angles (deg)	
E(2)–A–C*–E(3)	fixed at 176.6° for MeN(BMe ₂) ₂ fixed at 180.0° for MeB(NMe ₂) ₂
E(3)–A–E(2)–C ^f	τ (E(2)–A–E(3)–C ^f) – τ (E(3)–A–E(2)–C ^f) τ (E(3)–A–E(2)–C ^c) – τ (E(3)–A–E(2)–C ^f) τ (E(2)–A–E(3)–C ^c) – τ (E(2)–A–E(3)–C ^f) all methyl groups in fixed orientations

^a A = N and E = B and corresponds to MeN(BMe₂)₂; A = B and E = N and corresponds to MeB(NMe₂)₂.

lack of symmetry, the coordination geometries of the two B and the N atoms remain essentially planar; the sum of the three valence angles at each is 359.9°. The two dihedral angles τ (B–N–B–C^c) are no longer required to be equal: one of them is calculated to be about 11°; the other, twice as large.

The optimal structure of the corresponding bisaminoborane MeB(NMe₂)₂ was found to be similar to that of MeN(BMe₂)₂. See Table 4. The independent structure parameters and constraints employed during structure refinements of the two molecules to the GED data are described in Table 7.

Structure refinements of HN(BMe₂)₂, MeN(BMe₂)₂, and MeB(NMe₂)₂ proceeded without difficulties and led to good agreement between calculated and experimental intensities, as evidenced by the low *R*-factors listed in Table 5 and the good fit between the calculated and experimental radial distribution curves shown in Figure 3. The best values for bond distances and valence and dihedral angles in the three compounds are listed in Table 4.

When comparing structure parameters determined by GED with the calculated counterparts, one should keep in mind that while calculations yield equilibrium values

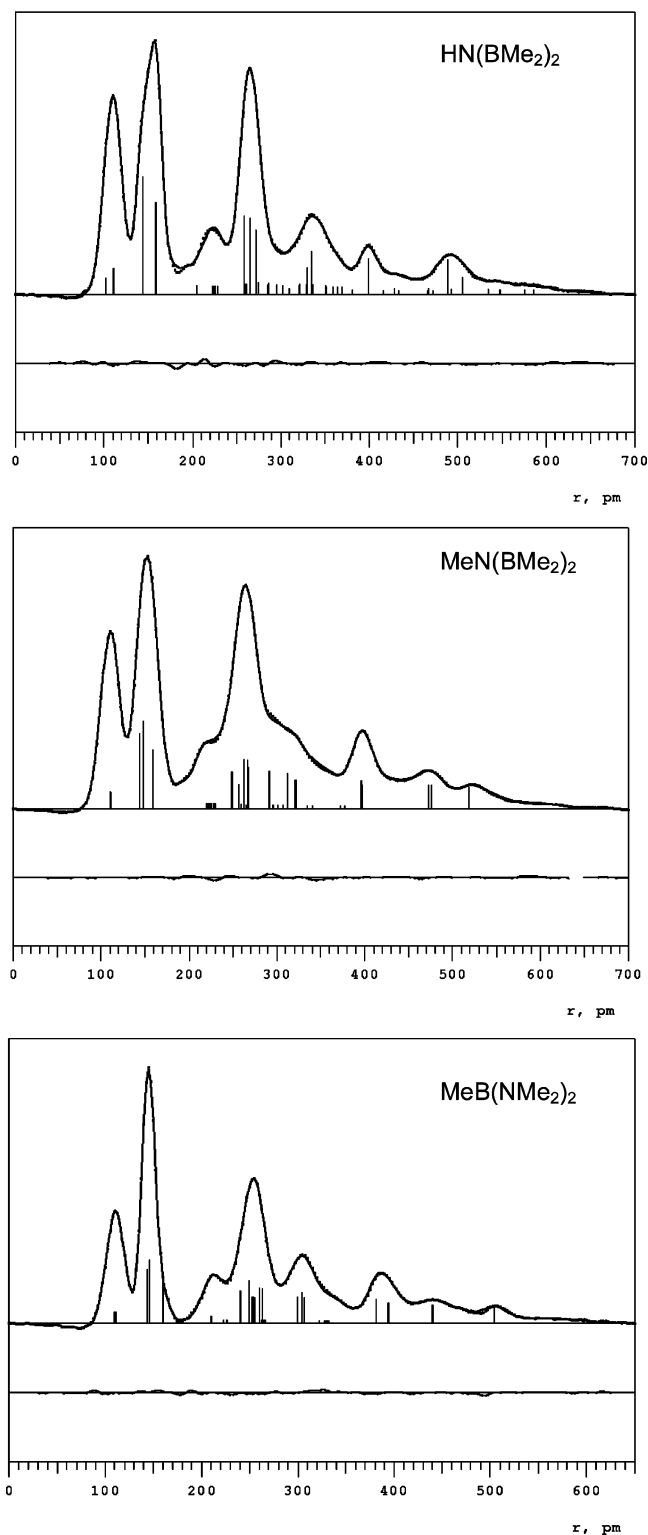
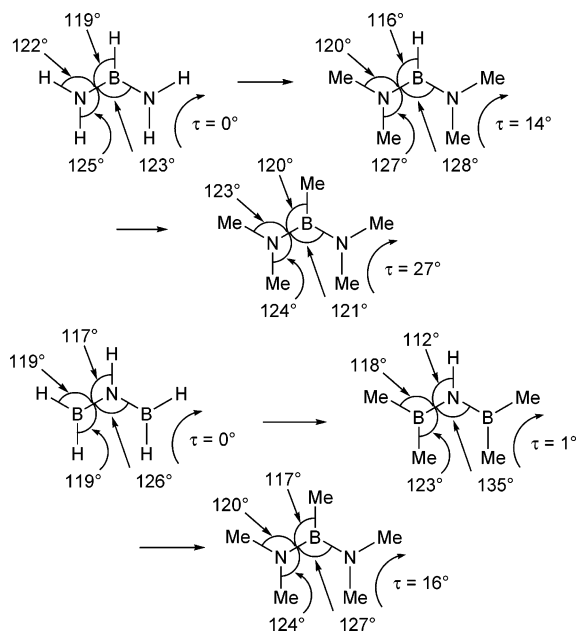


Figure 3. Experimental (dots) and calculated (lines) radial distribution curves of HN(BMe₂)₂, MeN(BMe₂)₂, and MeB(NMe₂)₂. Artificial damping constants are *k* = 12, 25, and 12 pm², respectively. Major interatomic distances are indicated by bars of height approximately equal to the area under the corresponding peak. Below: Difference curves.

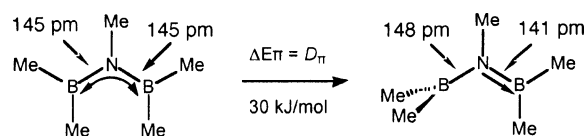
for bond distances and valence and dihedral angles, those obtained by GED have been averaged over thermal rotation and vibrations. The deviations between equilibrium and thermal average parameters are expected to be particularly large for C–H bond distances, A–C–H valence angles, and dihedral angles in general.

Scheme 5



The agreement between gas electron diffraction and DFT structure optimizations is, however, excellent with regard to those structure parameters that are defined by the positions of the “heavy atoms” N, B, and C. Thus, calculated and experimental N–B, N–C, or B–C bond distances agree to within 1.0 pm. If the calculated distances are uniformly reduced by 0.2 pm, they are all in agreement with their experimental counterparts to within the error limits (3 esd’s) of the latter. Calculated and experimental valence angles defined by N, B, and C atoms agree to within 1.1°; only in one case is the difference (slightly) greater than the error limits of the experimental value. Calculated and experimental values for the dihedral angles determining the orientations of the dimethylamino groups in HB(NMe₂)₂ and MeB(NMe₂)₂ or the dimethylboryl group in MeN(BMe₂)₂ all agree to within 2°; in each case the difference is smaller than the experimental uncertainty. The GED data thus confirm the reliability of the calculated structures presented in this article. Finally we determined the total π -bonding energies (ΔE_{π}) and the mean N–B π -bond rupture energies (D_{π}) in HB(NMe₂)₂ and MeB(NMe₂)₂ by optimizing orthogonal models of C_{2v} and C_s symmetry, respectively. The total π -bonding energies and the mean π -bond rupture energies in HN(BMe₂)₂ and MeN(BMe₂)₂ were estimated in the same manner as for HN(BH₂)₂. The results are listed in Table 4. We now compare the structures of the three bisaminoboranes. Replacement of four H atoms in HB(NH₂)₂ by methyl groups to form HB(NMe₂)₂ without changing the planar structure or valence angles leads to a prohibitively short distance between the two C^c atoms: 279 pm as compared to the methyl group van der Waals diameter of 400 pm. The C^c...C^c distance is increased to 321 pm—and the strain partly relieved—by opening of the NBN and BNC^c valence angles and by internal rotation of the dimethylamino groups about the N–B bonds. See Scheme 5. The orthogonal forms of HB(NMe₂)₂ and the other compounds listed in Table 4 are characterized by much larger nongeminal Me...Me distances and are therefore relatively strain-free. Any strain introduced into the

Scheme 6



equilibrium structures would therefore reduce the calculated π -bonding energy ΔE_{π} . The total π -bonding energy in HB(NMe₂)₂, 200 kJ mol⁻¹, is in fact very similar to that of unsubstituted HB(NH₂)₂, 193 kJ mol⁻¹; the strain accompanying the introduction of methyl groups has clearly been canceled by their stabilizing inductive effect.

Replacement of the H atom at the central B in HB(NMe₂)₂ by a methyl group C^{*}H₃ without change of valence angles or the torsional angle τ (N–B–N–C^c) leads to prohibitively short distances between the C^{*} atom and the two C^c atoms (about 287 pm). The repulsive strain is partially relieved by opening of the NBC^{*} and BNC^t valence angles. See Scheme 5. The opening of these angles is, however, accompanied by a closing of the \angle NBN and \angle NBC^c angles, which in turn leads to a decrease of the C^c...C^c distance. Both C^{*}...C^t and C^c...C^c repulsive strains are relieved by an increase of the torsional angle τ (NBNC^c) from 14° to 27°: in the equilibrium structure both the C^c...C^c and the two C^{*}...C^t distances are equal to or greater than 300 pm. The introduction of the fifth methyl group reduces the total π -bonding energy from 200 to 164 kJ mol⁻¹. In this case the added strain and the inductive effect of a more electron releasing substituent at the B atom act in the same direction.

Comparison of the structures of the three bisborylamines reveals a slightly different pattern. The transformation of HN(BH₂)₂ into HN(BMe₂)₂ through the addition of four methyl groups leads to an opening of the BNB and NBC^c valence angles, but the resulting angle at the bridgehead atom (\angle BNB) is much larger than in the corresponding bisaminoborane, and the torsional angle τ (BNBC^c) (1°) is negligible. See Scheme 5. In this case, the added steric strain combines with the unfavorable inductive effect of more electron releasing substituents at the B atom to reduce the total π -bonding energy by 30 kJ mol⁻¹ relative to HN(BH₂)₂.

Replacement of the H atom at the bridgehead N in HN(BMe₂)₂ by a methyl group leads to a 8° reduction of \angle BNB and increases of the torsional angles of the two BMe₂ groups to about 10° and 20°, respectively. ΔE_{π} is reduced by 22 kJ mol⁻¹; a favorable inductive effect is clearly swamped by steric strain.

Calculations on MeN(BMe₂)₂ show that the energy required to rupture *one* N–B π -bond in molecules with 2c or 3c π -bonding is considerably smaller than the *mean* π -bond rupture energy; optimization of a model with one BMe₂ group rotated into an orthogonal orientation yields a *one* π -bond rupture energy of D_{π} = 30 kJ mol⁻¹, as compared to the mean value of $\langle D_{\pi} \rangle$ = 72 kJ mol⁻¹. See Scheme 6.

Mean π -Bond Rupture Energies and N–B Bond Distances. Above we have calculated the mean π -bond rupture energies and N–B bond distances in four aminoboranes, three bisaminoboranes, three bisborylamines, two trisaminoboranes, and two trisbory-

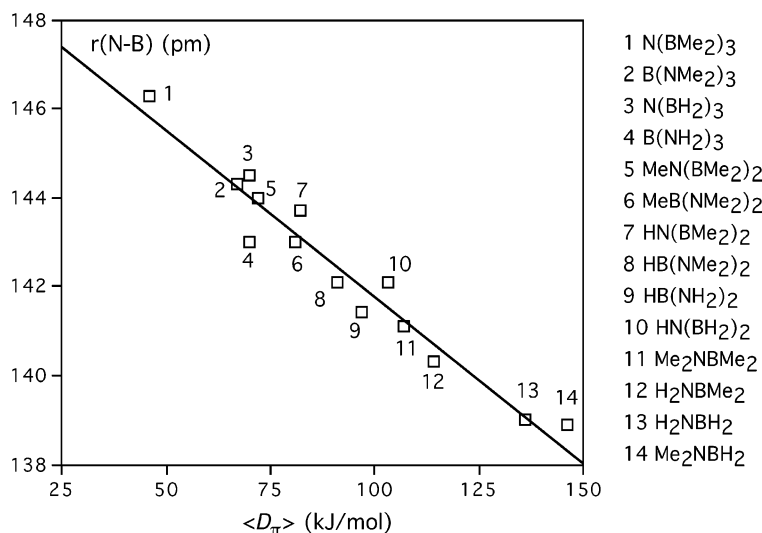


Figure 4. (Left) Variation of N–B bond distances in the 14 boron–nitrogen compounds under consideration as a function of the mean π -bond rupture energy $\langle D_\pi \rangle$. (Right) List of the molecules numbered in the order of increasing π -bond rupture energy.

lamines. The mean π -bond rupture energies in the 14 compounds have been found to vary from 46 kJ mol^{-1} in $\text{N}(\text{BMe}_2)_3$ to 146 kJ mol^{-1} in Me_2NBH_2 , while the N–B bond distances vary from 146.3 pm in the former to 138.9 pm in the latter.

We have already noted the following:

(i) The mean π -bond rupture energies of the prototypical 4c,6e and 4c,2e systems, $\text{B}(\text{NH}_2)_3$ and $\text{N}(\text{BH}_2)_3$, respectively, differ by less than 1 kJ mol^{-1} , while the mean π -bond rupture energies of the prototypical 3c,4e and 3c,2e systems, $\text{HB}(\text{NH}_2)_2$ and $\text{HN}(\text{BH}_2)_2$, respectively, differ by less than 6 kJ mol^{-1} . In these systems the mean π -bond strength is determined by the number of centers, not by the number of π -electron pairs.

(ii) The mean π -bond rupture energies of the simplest 2c system, H_2NBH_2 , in the simplest 3c systems, $\text{HB}(\text{NH}_2)_2$ and $\text{HN}(\text{BH}_2)_2$, and in the simplest 4c systems, $\text{B}(\text{NH}_2)_3$ and $\text{N}(\text{BH}_2)_3$, vary in the order 4.0:3.0:2.0.

(iii) When H atoms at an acceptor atom (B) are replaced by more electron releasing methyl groups, the mean π -bond rupture energy is significantly reduced due to a combination of inductive effects and increased steric strain. When H atoms at a donor atom (N) are replaced by methyl groups, the effect on the π -bond rupture energy is determined by the balance of inductive effects and steric strain. If the former dominates, the π -bond energy increases; if the latter dominates, it is reduced. The magnitude of the change is, however, much smaller than for substitution at the acceptor atom.

(iv) A plot of N–B bond distances as a function of $\langle D_\pi \rangle$ is shown in Figure 4. There is a clear trend of decreasing bond distance with increasing π -bond rupture energy, and linear regression analysis yields the relationship

$$R(\text{N-B}) = 149.3 \text{ pm} - [0.075 \text{ pm mol kJ}^{-1}] \langle D_\pi \rangle \quad (1)$$

with linear correlation coefficient $\rho = 0.97$. The average deviation between the bond distance obtained by DFT structure optimization and that estimated from eq 1 is 0.3 pm, and the maximum deviation, 1.1 pm, is found for compound no. 4, $\text{B}(\text{NH}_2)_3$.

We are somewhat surprised that the correlation between $R(\text{N-B})$ and $\langle D_\pi \rangle$ is so strong: the N–B bond

distance in the equilibrium structure is presumably determined by the strength of both π - and σ -bonding. The high correlation coefficient indicates that the variation of dative π -bond strength among the 14 compounds is greater than the variation of σ -bond strength. Comparison of the N–B bond distances and π -bond rupture energies of $\text{B}(\text{NH}_2)_3$ and $\text{N}(\text{BH}_2)_3$ (molecules no. 3 and 4) and of the bond distances and π -bond energies of $\text{HB}(\text{NH}_2)_2$ and $\text{HN}(\text{BH}_2)_2$ (molecules no. 10 and 9) suggests, however, that the σ -bonds in $\text{B}(\text{NH}_2)_3$ and $\text{HB}(\text{NH}_2)_2$ are stronger than those in $\text{N}(\text{BH}_2)_3$ and $\text{HN}(\text{BH}_2)_2$, respectively.

The relationship between N–B bond distance and the mean π -bond rupture energy appears to deviate from linearity for $\langle D_\pi \rangle$ less than 50 kJ mol^{-1} ; extrapolation of eq 1 to $\langle D_\pi \rangle = 0$ yields $R(\text{N-B}) = 149.3 \text{ pm}$, while the average N–B bond distance in the orthogonal forms of the 14 molecules (where $\langle D_\pi \rangle$ is zero by definition) is 147.8 pm.

Computational and Experimental Section

Density Functional Theory (DFT) Calculations. All DFT calculations were carried out using the GAUSSIAN-94/98 program systems with standard 6-311++G** basis sets for all atoms^{28,29} and with the B3PW91 functional that incorporates the exchange functional of Becke³⁰ and the local and nonlocal correlation functionals of Vosko, Wilk, and Nusair and of Perdew and Wang, respectively.^{31,32} Each structure optimization was followed by calculation of the Hessian matrix to ensure that a minimum (or saddle point) on the potential energy surface had been reached. The Hessian matrices of $\text{HN}(\text{BMe}_2)_2$, $\text{MeN}(\text{BMe}_2)_2$, and $\text{MeB}(\text{NMe}_2)_2$ were transferred to

(27) Spek, L. L. The Euclid Package. In *Computational Crystallography*; Sayre, D., Ed.; Clarendon Press: Oxford, U.K., 1982.

(28) Frisch, M. J.; Trucks, G. W.; Schlegel, H. B.; Gill, P. M. W.; Johnson, B. G.; Robb, M. A.; Cheeseman, J. R.; Keith, T.; Petersson, G. A.; Montgomery, J. A.; Raghavachari, K.; Al-Laham, M. A.; Zakrzewski, V. G.; Ortiz, J. V.; Foresman, J. B.; Cioslowski, J.; Stefanov, B. B.; Nanayakkara, A.; Challacombe, M.; Peng, C. Y.; Ayala, P. Y.; Chen, W.; Wong, M. W.; Andres, J. L.; Replogle, E. S.; Gomperts, R.; Martin, R. L.; Fox, D. J.; Binkley, J. S.; Defrees, D. J.; Baker, J.; Stewart, J. P.; Head-Gordon, M.; Gonzalez, C.; Pople, J. A. *Gaussian 94, Revision D.2*; Gaussian, Inc.: Pittsburgh, PA, 1995.

the program ASYM40³³ and transformed to scaled symmetrized force fields as described in refs 1 and 9. Diagonal C–H stretch force constants were multiplied by 0.900; all other diagonal force constants, by 0.943. Normal coordinate analysis yielded vibrational frequencies and their potential energy distribution (PED) as well as the root-mean-square amplitudes and vibrational correction terms needed for the GED structure refinements. See the Supporting Information.

Gas Electron Diffraction. Pure samples of HN(BMe₂)₂ and MeN(BMe₂)₂ were prepared by reacting Me₂BBr with the disilazane HN(SiEtMe₂)₂ or MeN(SiMe₃)₂, respectively, and characterized by ¹H and ¹¹B NMR spectroscopy as described by Nöth and Vahrenkamp.^{34,35} The sample of MeB(NMe₂)₂ was a gift from K. Niedenzu. It had been prepared by a ligand exchange reaction of B(NMe₂)₃ with BCl₃ to form ClB(NMe₂)₂, followed by reaction with the Grignard reagent MeMgI, and fully characterized by ¹H, ¹¹B, and ¹³C NMR as well as IR and Raman spectroscopy.^{36,37} The electron diffraction data for HN(BMe₂)₂ and MeN(BMe₂)₂ were recorded on the Oslo electron diffraction unit;³⁸ those of MeB(NMe₂)₂, on our Balzers KDG2 unit.³⁹ Relevant information about the experiments is summarized in Table 5. Atomic scattering factors were taken from ref 40. Backgrounds were drawn as least-squares-adjusted ninth degree polynomials to the difference between the total experimental and calculated molecular intensities using the background program PBG.⁹

Structure Refinements. Structure refinements were carried out by least-squares calculations on the molecular intensities using the program PLSQ.⁹ Corrections for thermal motion were carried out by the *B*–*I* scheme described in refs 9 and 25. Bonded and nonbonded distances between the “heavy atoms” B, N, and C were corrected for thermal motion, and distances involving H atoms were not. Vibrational amplitudes corresponding to related distances between bonded or nonbonded atoms were collected in groups and refined with constant differences. Nonrefined vibrational amplitudes were fixed at the calculated values. The estimated standard deviations obtained with diagonal weight matrices were multiplied by a factor of 1.5 to compensate for data correlation and further expanded to include an estimated scale uncertainty of 0.1%.

HN(BMe₂)₂. Under *C*₂ symmetry the structure of the NB₂C₄ frame of the molecule is determined by eight independent

parameters, i.e., three bond distances, three valence angles, and two dihedral angles. Specification of the structures of the methyl groups requires 18 more. To reduce the number of parameters to be refined, we fixed all differences between individual C–H bond distances and all differences between individual B–C–H valence angles, at the values obtained by the DFT calculations; only the mean C–H bond distance and the mean B–C–H angle were refined. The dihedral angles determining the orientation of the C^c methyl groups were fixed at the calculated values, and one dihedral angle determining the orientation of the C^c methyl groups was refined. The thermal average value thus obtained, 25(2)°, is close to the average of the values corresponding to eclipsed (0°) and staggered (60°) orientations. The number of parameters determining the structure of the frame was reduced to five by fixing the two dihedral angles τ(B–N–B–C^c) and τ(B–N–B–C^c) and the difference between the B–C^c and B–C^c bond distances at the calculated values. Least-squares refinement of the eight independent structure parameters listed in Table 6, along with eight vibrational amplitude parameters, yielded the best values listed in Table 4.

MeN(BMe₂)₂. Due to the lack of molecular symmetry, specification of the structure of the CNB₂C₄ frame requires no less than 15 independent parameters, while description of the structures of the methyl groups requires 60 more. The number of parameters used to describe the structure of the frame was reduced to seven by introducing the constraints listed in Table 7. For the methyl groups only two independent parameters were refined, viz., the mean C–H bond distance and the mean (N/B)–C–H valence angle. Least-squares refinement of the nine independent structure parameters listed in Table 7, along with 10 vibrational amplitude parameters, yielded the structure parameters listed in Table 4.

MeB(NMe₂)₂. MeB(NMe₂)₂ is isostructural with MeN(BMe₂)₂, and the independent structure parameters were defined in a completely analogous fashion. The constraints imposed during the structure refinements were also analogous except in one respect: while the coordination geometry of the N atom in the bisborylamine was restricted to a small deviation from planarity by fixing the dihedral angle τ(B(2)–N–C(20)–B(3)) at the calculated value of 176.6°, the coordination geometry of the B atom in the bisaminoborane was assumed to be strictly planar as predicted by the DFT calculations. See Table 7. Refinement of nine independent structure parameters, along with nine amplitude parameters, yielded the best values listed in Table 4.

Acknowledgment. We are grateful to professor K. Niedenzu for the sample of MeB(NMe₂)₂, and to cand. real. Arne Almenningsen, Mr. Hans V. Volden, and Ms. Snefrid Gundersen for technical assistance.

Supporting Information Available: Figure S1, Molecular model of MeB(NMe₂)₂; Figure S2, Gas electron diffraction intensity curves for HN(BMe₂)₂, MeN(BMe₂)₂, and MeB(NMe₂)₂; Table S1, MeB(NMe₂)₂, definition of internal coordinates; Table S2, MeB(NMe₂)₂, symmetry coordinates; Table S3, MeB(NMe₂)₂, frequencies and descriptions of the normal vibrational modes of the CB(NC₂)₂ framework; Table S4, MeB(NMe₂)₂, interatomic distances, vibrational amplitudes, and shrinkages of the CB(NC₂)₂ framework; Table S5, HN(BMe₂)₂ and MeN(BMe₂)₂, approximate description of normal coordinates in terms of symmetry coordinates; Table 6, HN(BMe₂)₂ and MeN(BMe₂)₂, frequencies and descriptions of the normal vibrational modes of the molecular frameworks; Table 7, HN(BMe₂)₂, interatomic distances, vibrational amplitudes, and shrinkages of the N(BC₂)₂ framework; Table 8, MeN(BMe₂)₂, interatomic distances, vibrational amplitudes and shrinkages of the N(BC₂)₂ framework. This material is available free of charge via the Internet at <http://pubs.acs.org>.

OM050476X

(29) Frisch, M. J.; Trucks, G. W.; Schlegel, H. B.; Scuseria, G. E.; Robb, M. A.; Cheeseman, J. R.; Zakrzewski, V. G.; Montgomery, J. A., Jr.; Stratmann, R. E.; Burant, J. C.; Dapprich, S.; Millam, J. M.; Daniels, A. D.; Kudin, K. N.; Strain, M. C.; Farkas, O.; Tomasi, J.; Barone, V.; Cossi, M.; Cammi, R.; Mennucci, B.; Pomelli, C.; Adamo, C.; Clifford, S.; Ochterski, J.; Petersson, G. A.; Ayala, P. Y.; Cui, Q.; Morokuma, K.; Malick, D. K.; Rabuck, A. D.; Raghavachari, K.; Foresman, J. B.; Cioslowski, J.; Ortiz, J. V.; Baboul, A. G.; Stefanov, B. B.; Liu, G.; Liashenko, A.; Piskorz, P.; Komaromi, I.; Gomperts, R.; Martin, R. L.; Fox, D. J.; Keith, T.; Al-Laham, M. A.; Peng, C. Y.; Nanayakkara, A.; Challacombe, M.; Gill, P. M. W.; Johnson, B.; Chen, W.; Wong, M. W.; Andres, J. L.; Gonzalez, C.; Head-Gordon, M.; Replogle, E. S.; Pople, J. A. *Gaussian 98, Revision A.9*; Gaussian, Inc.: Pittsburgh, PA, 1998.

(30) Becke, A. D. *Phys. Rev. A* **1988**, *38*, 3098.

(31) Vosko, S. H.; Wilk, L.; Nusair, M. *Can. J. Phys.* **1980**, *58*, 1200.

(32) Burke, K.; Perdew, J. P.; Wang, Y. In *Electronic Density Functional Theory: Recent Progress and New Directions*; Dobson, J. F., Vignale, G., Das, M. P., Eds.; Plenum Press: New York, 1998.

(33) Hedberg, L.; Mills, I. M. *J. Mol. Spectrosc.* **2000**, *203*, 82.

(34) Vahrenkamp, H. Ph.D. Thesis, University of München, 1967.

(35) Nöth, H.; Vahrenkamp, H. *J. Organomet. Chem.* **1969**, *16*, 357.

(36) Niedenzu, K.; Dawson, J. W. *Boron–Nitrogen Compounds*; Springer: Berlin, 1965.

(37) Blick, K. E.; Emerick, D. P.; Niedenzu, K.; Weber, W. Z. *Anorg. Allg. Chem.* **1981**, *473*, 153.

(38) Bastiansen, O.; Hassel, O.; Risberg, E. *Acta Chem. Scand.* **1955**, *9*, 232.

(39) Zeil, W.; Haase, J.; Wegmann, L. *Z. Instrumentenk.* **1966**, *74*, 84.

(40) Ross, A. W.; Fink, M. *J. Chem. Phys.* **1986**, *85*, 6810. Ross, A. W.; Fink, M.; Hilderbrandt, R. In *International Tables for Crystallography*; Wilson, A. J. C., Ed.; Kluwer Academic Publishers: Dordrecht, The Netherlands, 1992; Vol. C, p 245.